International Journal of Solids and Structures 72 (2015) 88–97

Contents lists available at ScienceDirect

International Journal of Solids and Structures

journal homepage: www.elsevier.com/locate/ijsolstr

Design, analysis and experimental investigation of three-dimensional structures with inertial amplification induced vibration stop bands

S. Taniker, C. Yilmaz *

Department of Mechanical Engineering, Bogazici University, 34342 Bebek, Istanbul, Turkey

ARTICLE INFO

Article history:
Received 3 December 2014
Received in revised form 13 May 2015
Available online 22 July 2015

Keywords:
Phononic band gaps
Phononic crystals
Inertial amplification
Three-dimensional lattice
3D printer

ABSTRACT

Three-dimensional (3D) phononic band gap structures are formed using identical inertial amplification mechanisms. The resonance and antiresonance frequencies that characterize the first vibration stop band of the building block mechanism are obtained analytically and by finite element method. The mechanism is optimized to yield wide vibration stop bands in two different 3D structures, namely, an octahedron and a 2×3 array of octahedrons. Furthermore, these structures are manufactured using a 3D polymer printer and their experimental frequency responses are obtained. Structural damping is added to the finite element model in order to match the resonant peak magnitudes of the numerical and experimental frequency response results. It is demonstrated that the 3D structures are capable of isolating excitations in longitudinal and two transverse directions in a very wide frequency range.

1. Introduction

A phononic band gap structure can impede propagation of acoustic or elastic waves in certain frequency ranges known as band gaps or stop bands. Stop bands can be generated in both infinite and finite periodic structures. There is no wave propagation within the stop band of an infinite periodic structure (Kushwaha, 1996). However, finite periodic structures cannot completely hinder wave propagation or vibration transmission even if they are excited within stop bands. The amount of vibration transmission in finite periodic structures can be characterized by analyzing the depth profile of the gap (stop band) in a frequency response function (FRF) plot (Yu et al., 2012; Shen et al., 2009). Finite periodic band gap structures can be used as noise or vibration isolators, mechanical filters, acoustic lenses or elastic waveguides (Xiuchang et al., 2011; Sun and Wu, 2007; Cervera et al., 2001; Hussein et al., 2007). Hence, designing phononic band gap structures with wide stop bands and obtaining good isolation characteristics inside the stop bands can be beneficial for various applications.

Band gaps (stop bands) in periodic structures are predominantly formed by means of Bragg scattering or local resonances. In the Bragg scattering method, generally, scatterers of high density material are embedded in a low density host material to create band gaps (Economou and Sigalas, 1994; Sprik and Wegdam, 1998; Kushwaha et al., 1998; Suzuki and Yu, 1998; Sainidou et al., 2002; Liu et al., 2000a; Wang et al., 2009; Wang et al., 2008; Wang et al., 2010; Hsieh et al., 2006; Kafesaki et al., 1995; Zhang et al., 2003; Robillard et al., 2009; Liu and Hussein, 2012). Oftentimes, face-centered cubic (FCC) arrangement of the scatterers are utilized to form band gaps (Economou and Sigalas, 1994; Sprik and Wegdam, 1998; Kushwaha et al., 1998; Suzuki and Yu, 1998; Sainidou et al., 2002; Liu et al., 2000a; Wang et al., 2009). Other arrangements such as simple cubic (SC), body-centered cubic (BCC) and hexagonal-close-packed (HCP) are also investigated (Wang et al., 2010; Hsieh et al., 2006; Kafesaki et al., 1995; Zhang et al., 2003). In some studies, band structures of the lattices are tuned by utilizing piezoelectricity (Wang et al., 2009; Wang et al., 2008; Wang et al., 2010) or magnetic fields (Robillard et al., 2009). In the local resonance method, band gaps are engendered with the addition of periodic local resonators to a host structure. To obtain band gaps at much lower frequencies than that can be obtained by Bragg scattering, high density materials are coated with soft elastic layers and embedded in a matrix material (Liu and Hussein, 2012; Jensen, 2003; Goffaux and Sánchez-Dehesa, 2003; Hirsekorn et al., 2004; Wang et al., 2004; Zhu et al., 2014; Baravelli and Ruzzene, 2013; Liu et al., 2000b; Gang et al., 2006). One-dimensional (1D) and two-dimensional (2D) periodic band gap structures are investigated in Liu and Hussein (2012), Jensen (2003), Goffaux and Sánchez-Dehesa (2003), Hirsekorn et al. (2004), Wang et al. (2004), Zhu et al. (2014) and Baravelli and Ruzzene (2013) and three-dimensional (3D) structures are studied in Liu et al. (2000b) and Gang et al. (2006).

* Corresponding author.
E-mail addresses: semih.taniker@boun.edu.tr (S. Taniker), cetin.yilmaz@boun.edu.tr (C. Yilmaz).

http://dx.doi.org/10.1016/j.ijsolstr.2015.07.013
0020-7683/

A novel band gap generation method is inertial amplification. In this method, a band gap is created with the amplification of a small mass by using displacement amplification mechanisms. Advantage of the inertial amplification method is to obtain wide low-frequency band gaps without increasing the total mass or decreasing the total stiffness of the lattice (Yilmaz et al., 2007; Yilmaz and Hulbert, 2010; Acar and Yilmaz, 2013; Taniker and Yilmaz, 2013a,b).

The inertial amplification method is implemented to SC, BCC and FCC structures in Taniker and Yilmaz (2013a,b). However, in those studies, only lumped parameter models are used. In this paper, 3D structures will be formed by utilizing identical distributed parameter inertial amplification mechanisms. The building block mechanism will be optimized to obtain the widest band gap and an octahedron structure and a 3D periodic structure will be formed. In order to obtain their frequency responses computationally, these structures will be analyzed by finite element method. Moreover, these structures will be manufactured and experimental modal analysis will be conducted to attain their experimental frequency responses.

2. Analytical and computational model

2.1. Analytical model

3D truss-like phononic band gap structures are investigated in this study. The inertial amplification mechanism shown in Fig. 1(a) will be the building block of these 3D structures. Here, thicknesses of the second and fourth segments are small, hence they act like flexure hinges.

In Acar and Yilmaz (2013), it was shown that a vibration stop band is formed between the first two natural frequencies of an inertial amplification mechanism. Moreover, the first antiresonance frequency of the mechanism determines the stop band depth. Therefore, these natural frequencies need to be calculated for the inertial amplification mechanism shown in Fig. 1(a). Fig. 1(b)–(d) shows the first three vibration modes of the inertial amplification mechanism. In Acar and Yilmaz (2013), a similar mechanism was used to form a 2D phononic band gap structure. However, in this study, the third segment shown in Fig. 1(a) has trapezoidal shape whereas it was in rectangular shape in Acar and Yilmaz (2013). Therefore, kinetic energies of the vibration modes will be different than those in Acar and Yilmaz (2013). However, potential energy calculations are based on the properties of the thin beam sections (second and fourth) and the calculations in Acar and Yilmaz (2013) can be used.

In the first mode, trapezoid's center of mass will translate more compared to that of a rectangle, which increases the kinetic energy in this mode, that in turn reduces its natural frequency. On the other hand, in the second and third modes, trapezoid's center of mass will translate less compared to that of a rectangle, which decreases the kinetic energy in these modes, that in turn increases their natural frequencies. As the first stop band will be formed between the first two natural frequencies of the mechanism (Acar and Yilmaz, 2013), trapezoidal shaped third segments will enable a wider stop band.

Inertia of the third beam segment need to be determined for kinetic energy calculations. In Fig. 1, l_i and t_i are length and thickness of the ith beam for $i = 1, 2, 4$ and Fig. 2(a) shows the dimensions regarding the third beam segment. For the analytical calculations, l_{3A} in Fig. 2(a) is taken as zero, which gives that the third beam is in trapezoidal shape.

For the first mode seen in Fig. 2(b), the third beam rotates about the point O_1 in Fig. 2(a) and its inertia (I_{O_1}) is:

$$I_{O_1} = I_{O_1A} + I_{O_1B} \tag{1}$$

where

$$I_{O_1A} = m_{3A}\left(\frac{t_{3A}^2 + l_3^2}{12} + \left(\frac{l_3 + l_2}{2}\right)^2 + \left(\frac{t_{3A} - t_2}{2}\right)^2\right), \tag{2}$$

$$I_{O_1B} = m_{3B}\left(\frac{t_{3B}^2 + l_3^2}{18} + \left(\frac{2l_3}{3} + \frac{l_2}{2}\right)^2 + \left(\frac{t_{3B}}{3} + t_{3A} - \frac{t_2}{2}\right)^2\right) \tag{3}$$

and m_{3A} and m_{3B} are the masses of the sections denoted by A and B in Fig. 2.

Now, assuming small oscillations, total rotational kinetic energy of the third beam segments (four of them) can be obtained as in Acar and Yilmaz (2013).

$$T_r = 4 \times \frac{1}{2} I_{O_1} \dot{\alpha}^2 = 2 I_{O_1} \dot{\alpha}^2 \tag{4}$$

where

$$\alpha = \frac{x - y}{2t_3 - t_2 - t_4}. \tag{5}$$

Total translational kinetic energy of the first beam segments (two of them) and third beam segments (four of them) can be written as:

$$T_t = \frac{1}{2} m_1 \dot{x}^2 + \frac{1}{2} m_1 \dot{y}^2 + 4 \times \frac{1}{2} m_3 \left(\frac{\dot{x} + \dot{y}}{2}\right)^2. \tag{6}$$

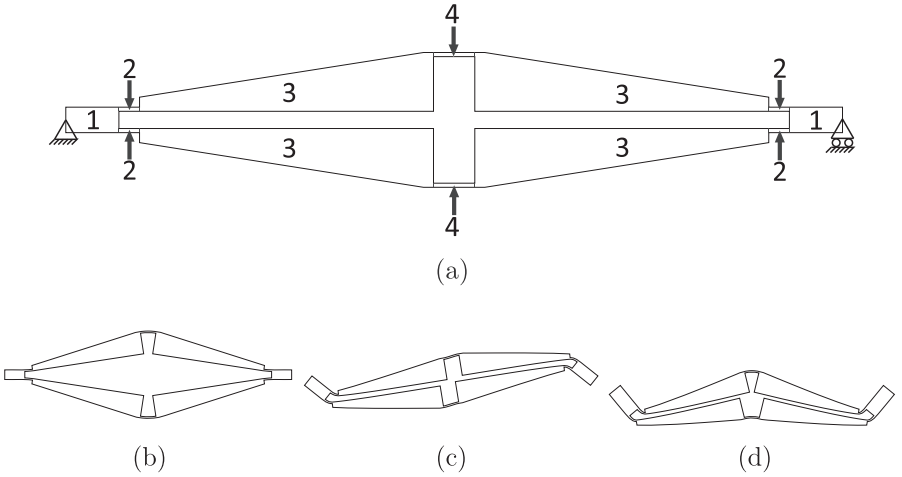

Fig. 1. (a) The inertial amplification mechanism, and its (b) first, (c) second and (d) third vibration modes. Here, the numbers represent different beam segments.